UCRL- 93362
PREPRINT

SUCCESSIVE REIGNITION OF FUEL-AIR MIXTURES AND PULSE COMBUSTION

Charles K. Westbrook
Lawrence Livermore National Laboratory
University of California
Livermore, CA 94550

This paper was prepared for submittal to
1985 Fall Meeting of the Western States
Section of The Combustion Institute
October 21-22, 1985
Davis, CA

September, 1985

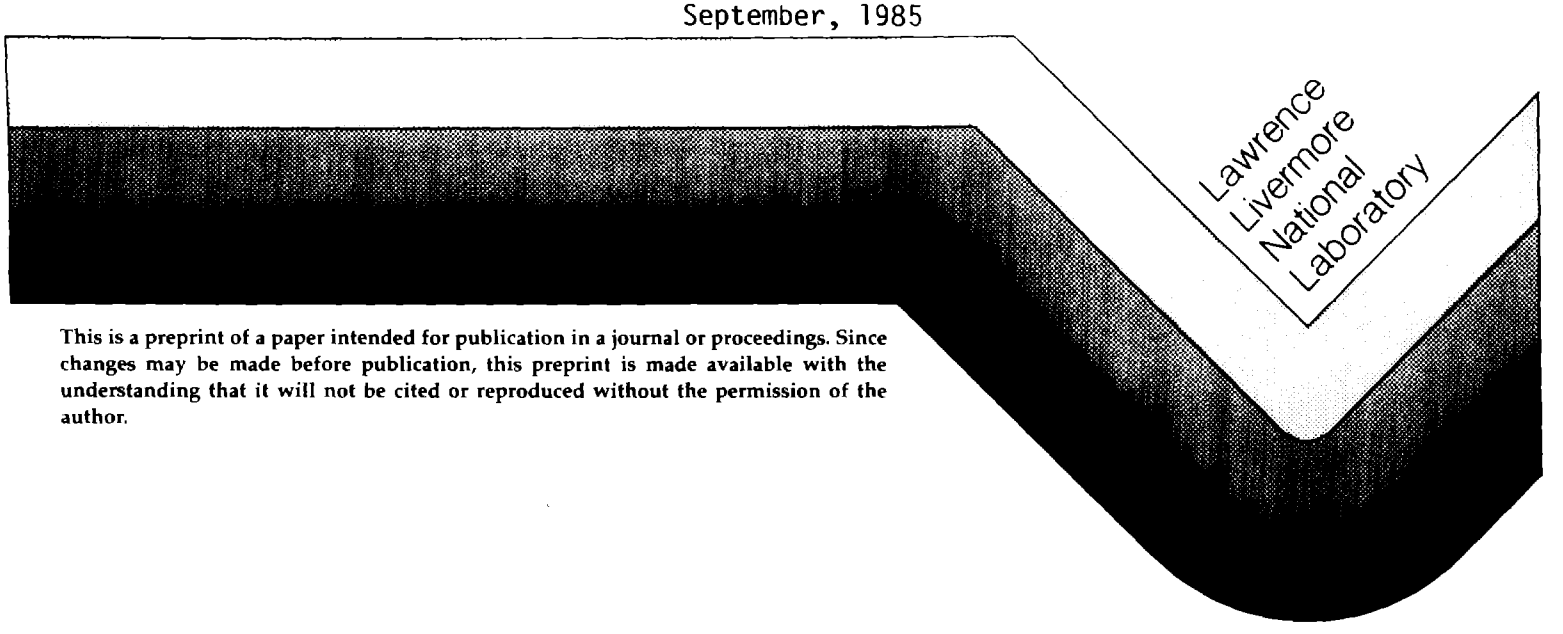

SUCCESSIVE REIGNITION OF FUEL-AIR MIXTURES AND PULSE COMBUSTION

Charles K. Westbrook

Lawrence Livermore National Laboratory

Abstract

Chemical kinetic modeling of the successive reignition of fuel-air mixtures is described, under conditions of pressure and temperature very similar to those encountered in conventional pulse combustion systems. The overall system model is described and the kinetic model is discussed in some detail. Computed results for ignition delay times are then related to time scales of interest in pulse combustion. From these comparisons, some of the physical and chemical factors which control the operation of the pulse combustor can be identified and quantified. In addition, the dependence of pulse combustor performance on various system parameters can be addressed, including the mass flow rate, fuel composition, presence of selected diluents and inhibitors, and combustion chamber geometry.

INTRODUCTION

The use of pulse combustors has been growing in recent years, primarily as a highly efficient home furnace unit fueled by natural gas. In addition to their high thermal efficiency, pulse combustors also produce significantly lower amounts of NO_x than conventional burners. Pulse combustors have been in existence for many years and have been used in a wide variety of applications. However, in spite of extensive practical experience with these systems, there is still very little theoretical understanding of the physical and chemical principles which govern the operation of pulse combustors.

Numerical modeling has provided a very powerful and versatile set of analytical tools for improving our understanding of combustion phenomena in recent years. An important part of this development has been a rapid

growth in the ability to simulate the detailed chemical kinetic processes which control the rate of combustion and heat release, as well as the formation rates of various chemical pollutants such as nitric oxide. In addition to aiding in the interpretation of existing laboratory data, a modeling approach can also be helpful by suggesting further experimental efforts which may be particularly productive.

In principle, any gaseous hydrocarbon fuel can be burned in a pulse combustion system, provided the fuel-oxidizer mixtures are indeed flammable and will ignite as discussed below. However, the emphasis of the present study is on the combustion of methane and natural gas. Current experimental basic research on pulse combustion at Battelle-Columbus Laboratories and at Georgia Institute of Technology, both supported by the Gas Research Institute, and at Sandia National Laboratories supported by the U.S. Department of Energy, is concerned primarily with methane and natural gas combustion. In addition, the dominant practical application area for pulse combustion at present is for natural gas-burning furnaces. The principles outlined below are sufficiently general to apply to other fuel-oxidizer mixtures, and examples of propane-air mixtures are discussed, but most of the work described concerns the oxidation of methane and natural gas.

NUMERICAL MODEL AND CHEMICAL KINETICS MECHANISMS

The numerical model employed for the calculations described in this paper is the HCT code [1] developed at LLNL. This program solves the coupled differential equations of conservation of mass, momentum, energy, and each chemical species, using finite difference techniques. Since the typical pulse combustor is an open system in which products are driven out through an exhaust pipe, the present calculations were carried out at a constant pressureof one atmosphere. Strictly speaking this is not quite true, with typical peak-to-peak pressure oscillations as high as 2 psi [2], but these pressure oscillations are driven by the heat release of the fuel ignition. The present modeling calculations describe only the fuel ignition during a short fraction of the entire cycle, and it is expected that the pressure will remain nearly uniform over this time interval.

The most important part of the numerical model is the detailed chemical kinetic reaction mechanism. In Table I the reaction mechanism is listed, showing both the forward and reverse reaction rates. This reaction mechanism has been developed over the past few years and documented in a series of publications [3-5]. With regard to natural gas combustion, this mechanism has been the basis for modeling studies that demonstrated the importance of the small quantities of minor hydrocarbon species present in natural gas, particularly the ethane [6] and propane [7] components. Because the mechanism is intended to describe natural gas combustion (as opposed to purely methane combustion), and because it has also been used to examine propane combustion in a pulse combustor, the mechanism in Table I

Table I
Fuel oxidation mechanism. Reaction rates in cm^3-mole-sec-kcal units, $k=AT^n\exp(-E_a/RT)$

	Reaction	Forward rate			Reverse rate		
		log A	n	E_a	log A	n	E_a
1.	$H+O_2 \rightarrow O+OH$	14.27	0	16.79	13.17	0	0.68
2.	$H_2+O \rightarrow H+OH$	10.26	1	8.90	9.92	1	6.95
3.	$H_2O+O \rightarrow OH+OH$	13.53	0	18.35	12.50	0	1.10
4.	$H_2O+H \rightarrow H_2+OH$	13.98	0	20.30	13.34	0	5.15
5.	$H_2O_2+OH \rightarrow H_2O+HO_2$	13.00	0	1.80	13.45	0	32.79
6.	$H_2O+M \rightarrow H+OH+M$	16.34	0	105.00	23.15	-2	0.00
7.	$H+O_2+M \rightarrow HO_2+M$	15.22	0	-1.00	15.36	0	45.90
8.	$HO_2+O \rightarrow OH+O_2$	13.70	0	1.00	13.81	0	56.61
9.	$HO_2+H \rightarrow OH+OH$	14.40	0	1.90	13.08	0	40.10
10.	$HO_2+H \rightarrow H_2+O_2$	13.40	0	0.70	13.74	0	57.80
11.	$HO_2+OH \rightarrow H_2O+O_2$	13.70	0	1.00	14.80	0	73.86
12.	$H_2O_2+O_2 \rightarrow HO_2+HO_2$	13.60	0	42.64	13.00	0	1.00
13.	$H_2O_2+M \rightarrow OH+OH+M$	17.08	0	45.50	14.96	0	-5.07
14.	$H_2O_2+H \rightarrow HO_2+H_2$	12.23	0	3.75	11.86	0	18.70
15.	$O+H+M \rightarrow OH+M$	16.00	0	0.00	19.90	-1	103.72
16.	$O_2+M \rightarrow O+O+M$	15.71	0	115.00	15.67	-0.28	0.00
17.	$H_2+M \rightarrow H+H+M$	14.34	0	96.00	15.48	0	0.00
18.	$CO+OH \rightarrow CO_2+H$	7.11	1.3	-0.77	9.15	1.3	21.58
19.	$CO+HO_2 \rightarrow CO_2+OH$	14.18	0	23.65	15.23	0	85.50
20.	$CO+O+M \rightarrow CO_2+M$	15.77	0	4.10	21.74	-1	131.78
21.	$CO_2+O \rightarrow CO+O_2$	12.44	0	43.83	11.50	0	37.60
22.	$HCO+OH \rightarrow CO+H_2O$	14.00	0	0.00	15.45	0	105.15
23.	$HCO+M \rightarrow H+CO+M$	14.16	0	19.00	11.70	1	1.55
24.	$HCO+H \rightarrow CO+H_2$	14.30	0	0.00	15.12	0	90.00
25.	$HCO+O \rightarrow CO+OH$	14.00	0	0.00	14.46	0	87.90
26.	$HCO+HO_2 \rightarrow CH_2O+O_2$	14.00	0	3.00	15.56	0	46.04
27.	$HCO+O_2 \rightarrow CO+HO_2$	12.60	0	7.00	12.95	0	39.29
28.	$CH_2O+M \rightarrow HCO+H+M$	16.52	0	81.00	11.15	1	-11.77
29.	$CH_2O+OH \rightarrow HCO+H_2O$	12.88	0	0.17	12.41	0	29.99
30.	$CH_2O+H \rightarrow HCO+H_2$	14.52	0	10.50	13.42	0	25.17
31.	$CH_2O+O \rightarrow HCO+OH$	13.70	0	4.60	12.24	0	17.17
32.	$CH_2O+HO_2 \rightarrow HCO+H_2O_2$	12.00	0	8.00	11.04	0	6.59
33.	$CH_4+M \rightarrow CH_3+H+M$	17.15	0	88.40	11.45	1	-19.52
34.	$CH_4+H \rightarrow CH_3+H_2$	14.10	0	11.90	12.68	0	11.43
35.	$CH_4+OH \rightarrow CH_3+H_2O$	3.54	3.08	2.00	2.76	3.08	16.68
36.	$CH_4+O \rightarrow CH_3+OH$	6.33	2.21	6.48	4.55	2.21	3.92
37.	$CH_4+HO_2 \rightarrow CH_3+H_2O_2$	13.30	0	18.00	12.02	0	1.45
38.	$CH_3+HO_2 \rightarrow CH_3O+OH$	13.51	0	0.00	10.00	0	0.00
39.	$CH_3+OH \rightarrow CH_2O+H_2$	12.60	0	0.00	14.08	0	71.73
40.	$CH_3+O \rightarrow CH_2O+H$	14.11	0	2.00	15.23	0	71.63
41.	$CH_3+O_2 \rightarrow CH_3O+O$	13.68	0	29.00	14.48	0	0.73
42.	$CH_2O+CH_3 \rightarrow CH_4+HCO$	10.00	0.5	6.00	10.32	0.5	21.14
43.	$CH_3+HCO \rightarrow CH_4+CO$	11.48	0.5	0.00	13.71	0.5	90.47
44.	$CH_3+HO_2 \rightarrow CH_4+O_2$	12.00	0	0.40	13.88	0	58.59
45.	$CH_3O+M \rightarrow CH_2O+H+M$	13.70	0	21.00	9.00	1	-2.56
46.	$CH_3O+O_2 \rightarrow CH_2O+HO_2$	12.00	0	6.00	11.11	0	32.17
47.	$C_2H_6 \rightarrow CH_3+CH_3$	19.35	-1	88.31	12.95	0	0.00
48.	$C_2H_6+CH_3 \rightarrow C_2H_5+CH_4$	-0.26	4	8.28	10.48	0	12.50

Table I (continued)
Fuel oxidation mechanism. Reaction rates in
cm^3-mole-sec-kcal units, $k=AT^n\exp(-E_a/RT)$

	Reaction	Forward rate			Reverse rate		
		log A	n	E_a	log A	n	E_a
49.	$C_2H_6+H \rightarrow C_2H_5+H_2$	2.73	3.5	5.20	2.99	3.5	27.32
50.	$C_2H_6+OH \rightarrow C_2H_5+H_2O$	9.94	1.05	1.81	10.23	1.05	20.94
51.	$C_2H_6+O \rightarrow C_2H_5+OH$	14.04	0	7.85	13.32	0	12.72
52.	$C_2H_5+M \rightarrow C_2H_4+H+M$	15.30	0	30.00	10.62	0	-11.03
53.	$C_2H_5+O_2 \rightarrow C_2H_4+HO_2$	12.00	0	5.00	11.12	0	13.70
54.	$C_2H_4+C_2H_4 \rightarrow C_2H_5+C_2H_3$	14.70	0	64.70	14.17	0	-2.61
55.	$C_2H_4+M \rightarrow C_2H_2+H_2$	16.97	0	77.20	12.66	1	36.52
56.	$C_2H_4+M \rightarrow C_2H_3+H+M$	18.80	0	108.72	17.30	0	0.00
57.	$C_2H_4+O \rightarrow CH_3+HCO$	12.52	0	1.13	11.20	0	31.18
58.	$C_2H_4+O \rightarrow CH_2O+CH_2$	13.40	0	5.00	12.48	0	15.68
59.	$C_2H_4+H \rightarrow C_2H_3+H_2$	7.18	2	6.00	6.24	2	5.11
60.	$C_2H_4+OH \rightarrow C_2H_3+H_2O$	12.68	0	1.23	12.08	0	14.00
61.	$C_2H_4+OH \rightarrow CH_3+CH_2O$	12.30	0	0.96	11.78	0	16.48
62.	$C_2H_3+M \rightarrow C_2H_2+H+M$	14.90	0	31.50	11.09	1	-10.36
63.	$C_2H_3+O_2 \rightarrow C_2H_2+HO_2$	12.00	0	10.00	12.00	0	17.87
64.	$C_2H_2+M \rightarrow C_2H+H+M$	14.00	0	114.00	9.04	1	0.77
65.	$C_2H_2+O_2 \rightarrow HCO+HCO$	12.60	0	28.00	11.00	0	63.65
66.	$C_2H_2+H \rightarrow C_2H+H_2$	14.30	0	19.00	13.62	0	13.21
67.	$C_2H_2+OH \rightarrow C_2H+H_2O$	12.78	0	7.00	12.73	0	16.36
68.	$C_2H_2+OH \rightarrow CH_2CO+H$	11.51	0	0.20	12.50	0	20.87
69.	$C_2H_2+O \rightarrow C_2H+OH$	15.51	-0.6	17.00	14.47	-0.6	0.91
70.	$C_2H_2+O \rightarrow CH_2+CO$	13.83	0	4.00	13.10	0	54.67
71.	$C_2H+O_2 \rightarrow HCO+CO$	13.00	0	7.00	12.93	0	138.40
72.	$C_2H+O \rightarrow CO+CH$	13.70	0	0.00	13.50	0	59.43
73.	$CH_2+O_2 \rightarrow HCO+OH$	14.00	0	3.70	13.61	0	76.58
74.	$CH_2+O \rightarrow CH+OH$	11.28	0.68	25.00	10.77	0.68	25.93
75.	$CH_2+H \rightarrow CH+H_2$	11.43	0.67	25.70	11.28	0.67	28.72
76.	$CH_2+OH \rightarrow CH+H_2O$	11.43	0.67	25.70	11.91	0.67	43.88
77.	$CH+O_2 \rightarrow CO+OH$	11.13	0.67	25.70	11.71	0.67	185.60
78.	$CH+O_2 \rightarrow HCO+O$	13.00	0	0.00	13.13	0	71.95
79.	$CH_3OH+M \rightarrow CH_3+OH+M$	18.48	0	80.00	13.16	1	-10.98
80.	$CH_3OH+OH \rightarrow CH_2OH+H_2O$	12.60	0	2.00	7.27	1.66	25.31
81.	$CH_3OH+O \rightarrow CH_2OH+OH$	12.23	0	2.29	5.90	1.66	8.35
82.	$CH_3OH+H \rightarrow CH_2OH+H_2$	13.48	0	7.00	7.51	1.66	15.16
83.	$CH_3OH+H \rightarrow CH_3+H_2O$	12.72	0	5.34	12.32	0	36.95
84.	$CH_3OH+CH_3 \rightarrow CH_2OH+CH_4$	11.26	0	9.80	6.70	1.66	18.43
85.	$CH_3OH+HO_2 \rightarrow CH_2OH+H_2O_2$	12.80	0	19.36	7.00	1.66	11.44
86.	$CH_2OH+M \rightarrow CH_2O+H+M$	13.40	0	29.00	16.69	-0.66	7.58
87.	$CH_2OH+O_2 \rightarrow CH_2O+HO_2$	12.00	0	6.00	17.94	-1.66	28.32
88.	$C_2H_3+C_2H_4 \rightarrow C_4H_6+H$	12.00	0	7.30	13.00	0	4.70
89.	$C_2H_2+C_2H_2 \rightarrow C_4H_3+H$	13.00	0	45.00	13.18	0	0.00
90.	$C_4H_3+M \rightarrow C_4H_2+H+M$	16.00	0	60.00	11.92	1	2.54
91.	$C_2H_2+C_2H \rightarrow C_4H_2+H$	13.60	0	0.00	14.65	0	0.55
92.	$C_4H_2+M \rightarrow C_4H+H+M$	17.54	0	80.00	12.30	1.0	-16.40
93.	$C_2H_3+H \rightarrow C_2H_2+H_2$	13.30	0	2.50	13.12	0	68.08
94.	$C_3H_8 \rightarrow CH_3+C_2H_5$	16.23	0	84.84	10.18	1	-0.32
95.	$CH_3+C_3H_8 \rightarrow CH_4+iC_3H_7$	15.04	0	25.14	15.64	0	32.12
96.	$CH_3+C_3H_8 \rightarrow CH_4+nC_3H_7$	15.04	0	25.14	15.64	0	32.12

Table I (continued)
Fuel oxidation mechanism. Reaction rates in
cm^3-mole-sec-kcal units, $k=AT^n\exp(-E_a/RT)$

	Reaction	Forward rate log A	n	E_a	Reverse rate log A	n	E_a
99.	$iC_3H_7 \rightarrow H+C_3H_6$	13.80	0	36.90	13.00	0	1.50
100.	$iC_3H_7 \rightarrow CH_3+C_2H_4$	10.30	0	29.50	4.66	1	4.29
101.	$nC_3H_7 \rightarrow CH_3+C_2H_4$	13.98	0	31.00	8.34	1	5.79
102.	$nC_3H_7 \rightarrow H+C_3H_6$	14.10	0	37.00	13.00	0	1.50
103.	$iC_3H_7+C_3H_8 \rightarrow nC_3H_7+C_3H_8$	10.48	0	12.90	10.48	0	12.90
104.	$C_2H_3+C_3H_8 \rightarrow C_2H_4+iC_3H_7$	11.00	0	10.40	11.12	0	17.80
105.	$C_2H_3+C_3H_8 \rightarrow C_2H_4+nC_3H_7$	11.00	0	10.40	11.12	0	17.80
106.	$C_2H_5+C_3H_8 \rightarrow C_2H_6+iC_3H_7$	11.00	0	10.40	10.56	0	9.93
107.	$C_2H_5+C_3H_8 \rightarrow C_2H_6+nC_3H_7$	11.00	0	10.40	10.56	0	9.93
108.	$C_3H_8+O \rightarrow iC_3H_7+OH$	13.45	0	5.20	12.27	0	7.41
109.	$C_3H_8+O \rightarrow nC_3H_7+OH$	14.05	0	7.85	12.88	0	9.61
110.	$C_3H_8+OH \rightarrow iC_3H_7+H_2O$	8.68	1.4	0.85	8.93	1.25	22.37
111	$C_3H_8+OH \rightarrow nC_3H_7+H_2O$	8.76	1.4	0.85	9.01	1.25	22.37
112.	$C_3H_8+HO_2 \rightarrow iC_3H_7+H_2O_2$	12.70	0	18.00	12.01	0	8.43
113.	$C_3H_8+HO_2 \rightarrow iC_3H_7+H_2O_2$	12.70	0	18.00	12.01	0	8.43
114.	$C_3H_6+O \rightarrow C_2H_4+CH_2O$	13.77	0	5.00	13.76	0	86.67
115.	$iC_3H_7+O_2 \rightarrow C_3H_6+HO_2$	12.00	0	5.00	11.30	0	17.48
116.	$nC_3H_7+O_2 \rightarrow C_3H_6+HO_2$	12.00	0	5.00	11.30	0	17.48
117.	$C_3H_8+O_2 \rightarrow iC_3H_7+HO_2$	13.60	0	47.50	12.31	0	0.00
118.	$C_3H_8+O_2 \rightarrow nC_3H_7+HO_2$	13.60	0	47.50	12.31	0	0.00
119.	$C_3H_6+OH \rightarrow C_2H_5+CH_2O$	12.90	0	0.00	13.66	0	17.35
120.	$C_3H_6+O \rightarrow C_2H_5+HCO$	12.55	0	0.00	11.85	0	29.92
121.	$C_3H_6+OH \rightarrow CH_3+CH_3CHO$	11.54	0	0.00	11.44	0	20.40
122.	$C_3H_6+O \rightarrow CH_3+CH_3CO$	13.07	0	0.60	12.25	0	38.37
123.	$CH_3CHO+H \rightarrow CH_3CO+H_2$	13.60	0	4.20	13.25	0	23.67
124.	$CH_3CHO+OH \rightarrow CH_3CO+H_2O$	13.00	0	0.00	13.28	0	36.62
125.	$CH_3CHO+O \rightarrow CH_3CO+OH$	12.70	0	1.79	12.00	0	19.16
126.	$CH_3CHO+CH_3 \rightarrow CH_3CO+CH_4$	12.23	0	8.43	13.48	0	28.00
127.	$CH_3CHO+HO_2 \rightarrow CH_3CO+H_2O_2$	12.23	0	10.70	12.00	0	14.10
128.	$CH_3CHO \rightarrow CH_3+HCO$	15.85	0	81.78	9.58	1	0.00
129.	$CH_3CHO+O_2 \rightarrow CH_3CO+HO_2$	13.30	0.5	42.20	7.00	0.5	4.00
130.	$CH_3CO \rightarrow CH_3+CO$	13.48	0	17.24	11.20	0	5.97
131.	$C_3H_6+H \rightarrow C_3H_5+H_2$	12.70	0	1.50	12.18	0	17.70
132.	$C_3H_6+CH_3 \rightarrow C_3H_5+CH_4$	10.95	0	8.50	11.87	0	25.18
133.	$C_3H_6+C_2H_5 \rightarrow C_3H_5+C_2H_6$	11.00	0	9.20	5.00	0	56.77
134.	$C_3H_6+OH \rightarrow C_3H_5+H_2O$	12.60	0	0.00	7.18	0	69.69
135.	$C_3H_8+C_3H_5 \rightarrow iC_3H_7+C_3H_6$	11.60	0	16.20	11.30	0	6.50
136.	$C_3H_8+C_3H_5 \rightarrow iC_3H_7+C_3H_6$	11.60	0	16.20	11.30	0	6.50
137.	$C_3H_5 \rightarrow C_3H_4+H$	13.60	0	70.00	8.00	1	0.00
138.	$C_3H_5+O_2 \rightarrow C_3H_4+HO_2$	11.78	0	10.00	11.08	0	10.00
139.	$1C_4H_8 \rightarrow C_3H_5+CH_3$	19.18	-1	73.40	13.13	0	0.00
140.	$1C_4H_8 \rightarrow C_2H_3+C_2H_5$	19.00	-1	96.77	12.95	0	0.00
141.	$1C_4H_8+O \rightarrow CH_3CHO+C_2H_4$	13.11	0	0.85	12.32	0	85.10
142.	$1C_4H_8+O \rightarrow CH_3CO+C_2H_5$	13.11	0	0.85	12.37	0	38.15
143.	$1C_4H_8+OH \rightarrow CH_3CHO+C_2H_5$	13.00	0	0.00	12.97	0	19.93
144.	$1C_4H_8+OH \rightarrow CH_3CO+C_2H_6$	13.00	0	0.00	12.99	0	32.43

Table I (continued)
Fuel oxidation mechanism. Reaction rates in
cm^3-mole-sec-kcal units, $k=AT^n\exp(-E_a/RT)$

	Reaction	Forward rate log A	n	E_a	Reverse rate log A	n	E_a
145.	$C_3H_4+O \rightarrow CH_2O+C_2H_2$	12.00	0	0.00	12.03	0	81.73
146.	$C_3H_4+O \rightarrow HCO+C_2H_3$	12.00	0	0.00	10.47	0	30.82
147.	$C_3H_4+OH \rightarrow CH_2O+C_2H_3$	12.00	0	0.00	11.93	0	18.25
148.	$C_3H_4+OH \rightarrow HCO+C_2H_4$	12.00	0	0.00	11.77	0	33.81
149.	$C_3H_6 \rightarrow C_3H_5+H$	13.00	0	78.00	11.00	0	0.00
150.	$C_2H_2+O \rightarrow HCCO+H$	4.55	2.7	1.39	2.70	2.7	12.79
151.	$CH_2CO+H \rightarrow CH_3+CO$	13.04	0	3.40	12.38	0	40.20
152.	$CH_2CO+O \rightarrow HCO+HCO$	13.00	0	2.40	11.54	0	33.50
153.	$CH_2CO+OH \rightarrow CH_2O+HCO$	13.45	0	0.00	13.44	0	18.50
154.	$CH_2CO+M \rightarrow CH_2+CO+M$	16.30	0	60.00	10.66	0	0.00
155.	$CH_2CO+O \rightarrow HCCO+OH$	13.70	0	8.00	10.86	0	8.00
156.	$CH_2CO+OH \rightarrow HCCO+H_2O$	12.88	0	3.00	11.03	0	11.00
157.	$CH_2CO+H \rightarrow HCCO+H_2$	13.88	0	8.00	11.39	0	8.00
158.	$HCCO+OH \rightarrow HCO+HCO$	13.00	0	0.00	13.68	0	40.36
159.	$HCCO+H \rightarrow CH_2+CO$	13.70	0	0.00	13.82	0	39.26
160.	$HCCO+O \rightarrow HCO+CO$	13.53	0	2.00	13.92	0	128.26
161.	$C_3H_6 \rightarrow C_2H_3+CH_3$	15.80	0	85.80	10.00	1	0.00
162.	$C_3H_5+H \rightarrow C_3H_4+H_2$	13.00	0	0.00	13.00	0	40.00
163.	$C_3H_5+CH_3 \rightarrow C_3H_4+CH_4$	12.00	0	0.00	13.00	0	40.00
164.	$C_2H_6+O_2 \rightarrow C_2H_5+HO_2$	13.00	0	51.00	12.00	0	0.00
165.	$C_2H_6+HO_2 \rightarrow C_2H_5+H_2O_2$	11.48	0	11.50	11.23	0	2.39
166.	$CH_3+C_2H_3 \rightarrow CH_4+C_2H_2$	12.00	0	0.00	13.88	0	66.05
167.	$CH_3+C_2H_5 \rightarrow CH_4+C_2H_4$	11.90	0	0.00	12.91	0	66.89
168.	$C_2H_5+C_3H_5 \rightarrow C_3H_6+C_2H_4$	12.10	0	0.00	10.00	0	50.00
169.	$C_2H_5+C_2H_5 \rightarrow C_2H_6+C_2H_4$	12.60	0	0.00	12.60	0	60.00
170.	$CH_3OH+CH_2O \rightarrow CH_3O+CH_3O$	12.19	0	79.57	13.48	0	0.00
171.	$CH_2O+CH_3O \rightarrow CH_3OH+HCO$	10.43	0	3.00	8.47	0	13.37
172.	$CH_4+CH_3O \rightarrow CH_3OH+CH_3$	11.30	0	7.00	9.02	0	2.22
173.	$C_2H_6+CH_3O \rightarrow CH_3OH+C_2H_5$	11.48	0	7.00	10.23	0	9.67
174.	$C_3H_8+CH_3O \rightarrow CH_3OH+iC_3H_7$	11.48	0	7.00	10.23	0	9.67
175.	$C_3H_8+CH_3O \rightarrow CH_3OH+nC_3H_7$	11.48	0	7.00	10.23	0	9.67
176.	$C_4H_{10} \rightarrow C_2H_5+C_2H_5$	16.30	0	81.30	10.60	1	-2.94
177.	$C_4H_{10} \rightarrow nC_3H_7+CH_3$	17.00	0	85.40	10.51	1	-2.49
178.	$C_4H_{10}+O_2 \rightarrow pC_4H_9+HO_2$	13.40	0	49.00	12.40	0	-2.20
179.	$C_4H_{10}+O_2 \rightarrow sC_4H_9+HO_2$	13.60	0	47.60	12.61	0	-3.62
180.	$C_4H_{10}+H \rightarrow pC_4H_9+H_2$	7.75	2	7.70	12.96	0	14.46
181.	$C_4H_{10}+H \rightarrow sC_4H_9+H_2$	7.24	2	5.00	13.19	0	15.87
182.	$C_4H_{10}+OH \rightarrow pC_4H_9+H_2O$	9.94	1.05	1.81	10.17	1.05	23.33
183.	$C_4H_{10}+OH \rightarrow sC_4H_9+H_2O$	9.41	1.25	0.70	9.66	1.25	22.22
184.	$C_4H_{10}+O \rightarrow pC_4H_9+OH$	14.05	0	7.85	13.17	0	12.24
185.	$C_4H_{10}+O \rightarrow sC_4H_9+OH$	13.75	0	5.20	12.87	0	9.59
186.	$C_4H_{10}+CH_3 \rightarrow pC_4H_9+CH_4$	12.11	0	11.60	13.00	0	18.56
187.	$C_4H_{10}+CH_3 \rightarrow sC_4H_9+CH_4$	11.90	0	9.50	12.80	0	16.46
188.	$C_4H_{10}+C_2H_3 \rightarrow pC_4H_9+C_2H_4$	12.00	0	18.00	12.41	0	25.38
189.	$C_4H_{10}+C_2H_3 \rightarrow sC_4H_9+C_2H_4$	11.90	0	16.80	12.31	0	24.18
190.	$C_4H_{10}+C_2H_5 \rightarrow pC_4H_9+C_2H_6$	11.00	0	13.40	10.85	0	12.92
191.	$C_4H_{10}+C_2H_5 \rightarrow sC_4H_9+C_2H_6$	11.00	0	10.40	10.85	0	9.92
192.	$C_4H_{10}+C_3H_5 \rightarrow pC_4H_9+C_3H_6$	11.60	0	18.80	13.70	0	0.00

Table I (continued)
Fuel oxidation mechanism. Reaction rates in
cm^3-mole-sec-kcal units, $k=AT^n\exp(-E_a/RT)$

	Reaction	Forward rate			Reverse rate		
		log A	n	E_a	log A	n	E_a
193.	$C_4H_{10}+C_3H_5 \rightarrow sC_4H_9+C_3H_6$	11.90	0	16.80	13.70	0	0.00
194.	$C_4H_{10}+HO_2 \rightarrow pC_4H_9+H_2O_2$	12.85	0	19.40	12.46	0	0.00
195.	$C_4H_{10}+HO_2 \rightarrow sC_4H_9+H_2O_2$	12.85	0	17.00	12.46	0	0.00
196.	$C_4H_{10}+CH_3O \rightarrow pC_4H_9+CH_3OH$	11.48	0	7.00	10.09	0	9.18
197.	$C_4H_{10}+CH_3O \rightarrow sC_4H_9+CH_3OH$	11.78	0	7.00	10.39	0	9.18
198.	$pC_4H_9 \rightarrow C_2H_5+C_2H_4$	13.40	0	28.80	11.48	0	8.00
199.	$pC_4H_9 \rightarrow {}_1C_4H_8+H$	13.10	0	38.60	13.00	0	1.50
200.	$pC_4H_9+O_2 \rightarrow {}_1C_4H_8+HO_2$	12.00	0	2.00	11.29	0	15.85
201.	$sC_4H_9 \rightarrow {}_2C_4H_8+H$	12.70	0	37.90	13.00	0	1.50
202.	$sC_4H_9 \rightarrow {}_1C_4H_8+H$	13.30	0	40.40	13.00	0	1.50
203.	$sC_4H_9 \rightarrow C_3H_6+CH_3$	14.30	0	33.20	11.50	0	7.40
204.	$sC_4H_9+O_2 \rightarrow {}_1C_4H_8+HO_2$	12.00	0	4.50	11.29	0	18.35
205.	$sC_4H_9+O_2 \rightarrow {}_2C_4H_8+HO_2$	12.30	0	4.25	11.59	0	18.10
206.	${}_1C_4H_8 \rightarrow C_4H_7+H$	18.61	-1	97.35	13.70	0	0.00
207.	${}_2C_4H_8 \rightarrow C_4H_7+H$	18.61	-1	97.35	13.70	0	0.00
208.	${}_1C_4H_8+H \rightarrow C_4H_7+H_2$	13.70	0	3.90	10.00	0	13.99
209.	${}_2C_4H_8+H \rightarrow C_4H_7+H_2$	13.70	0	3.80	10.00	0	13.89
210.	${}_1C_4H_8+OH \rightarrow C_4H_7+H_2O$	12.68	0	1.23	12.68	0	26.47
211.	${}_2C_4H_8+OH \rightarrow C_4H_7+H_2O$	12.68	0	1.23	12.68	0	26.47
212.	${}_1C_4H_8+CH_3 \rightarrow C_4H_7+CH_4$	11.00	0	7.30	11.78	0	17.86
213.	${}_2C_4H_8+CH_3 \rightarrow C_4H_7+CH_4$	11.00	0	8.20	11.78	0	18.76
214.	${}_1C_4H_8+O \rightarrow C_3H_6+CH_2O$	12.70	0	0.00	12.14	0	81.33
215.	${}_2C_4H_8+O \rightarrow iC_3H_7+HCO$	12.78	0	0.00	11.35	0	25.81
216.	${}_2C_4H_8+O \rightarrow C_2H_4+CH_3CHO$	12.00	0	0.00	11.20	0	84.25
217.	${}_1C_4H_8+OH \rightarrow iC_3H_7+CH_2O$	13.26	0	0.00	13.29	0	13.23
218.	${}_2C_4H_8+OH \rightarrow C_2H_5+CH_3CHO$	13.41	0	0.00	13.39	0	19.93
219.	$C_4H_7+M \rightarrow C_4H_6+H+M$	14.08	0	49.30	13.60	0	1.30
220.	$C_4H_7+M \rightarrow C_2H_4+C_2H_3+M$	11.00	0	37.00	4.96	1	-3.44
221.	$C_4H_7+O_2 \rightarrow C_4H_6+HO_2$	11.00	0	0.00	10.06	0	-0.90
222.	$C_4H_7+H \rightarrow C_4H_6+H_2$	13.50	0	0.00	13.03	0	56.81
223.	$C_4H_7+C_2H_3 \rightarrow C_4H_6+C_2H_4$	12.60	0	0.00	13.06	0	57.71
224.	$C_4H_7+C_2H_5 \rightarrow C_4H_6+C_2H_6$	12.60	0	0.00	12.51	0	49.84
225.	$C_4H_7+C_2H_5 \rightarrow {}_1C_4H_8+C_2H_4$	11.70	0	0.00	11.93	0	56.33
226.	$C_4H_7+C_2H_5 \rightarrow {}_2C_4H_8+C_2H_4$	11.70	0	0.00	11.93	0	56.33
227.	$C_4H_7+C_3H_5 \rightarrow C_4H_6+C_3H_6$	12.80	0	0.00	10.00	0	50.00
228.	$C_4H_6 \rightarrow C_2H_3+C_2H_3$	19.60	-1	98.15	13.10	0	0.00
229.	$C_4H_6+OH \rightarrow C_2H_5+CH_2CO$	12.00	0	0.00	12.57	0	30.02
230.	$C_4H_6+OH \rightarrow C_3H_5+CH_2O$	12.00	0	0.00	6.54	0	71.06
231.	$C_4H_6+OH \rightarrow C_2H_3+CH_3CHO$	12.00	0	0.00	11.74	0	18.55
232.	$C_4H_6+O \rightarrow C_2H_4+CH_2CO$	12.00	0	0.00	11.80	0	94.34
233.	$C_4H_6+O \rightarrow C_3H_4+CH_2O$	12.00	0	0.00	12.03	0	79.05
234.	$C_5H_{10} \rightarrow CH_3+C_4H_7$	19.00	-1	81.55	13.40	0	0.00
235.	$C_5H_{10}+O \rightarrow {}_1C_4H_8+CH_2O$	12.00	0	0.00	11.41	0	85.43
236.	$C_5H_{10}+O \rightarrow C_3H_6+CH_3CHO$	12.00	0	0.00	10.62	0	88.01
237.	$C_5H_{10}+OH \rightarrow pC_4H_9+CH_2O$	12.00	0	0.00	12.01	0	50.00
238.	$C_5H_{10}+OH \rightarrow nC_3H_7+CH_3CHO$	12.00	0	0.00	11.22	0	50.00

includes submechanisms for the oxidation of fuels up to and including C_4 species. These modeling studies have shown that the presence of these higher alkanes has a considerable effect on the ignition properties of natural gas, which are of importance in the analysis of the pulse combustion research. In contrast, the presence of the higher alkanes has little effect on the computed flame properties of natural gas, including the flammability limits and burning velocities. Computational results from the applications of this mechanism to pulse combustion will be presented below, together with a description of the most important features of the detailed kinetic pathways and rates responsible for the observations.

MODEL ASSUMPTIONS

The operation of a typical pulse combustor is deceptively simple. The combustion chamber has a relatively long exhaust pipe which is open to the atmosphere and whose length and volume largely determine the frequency of pulsation of the combustor. During each cycle, the heat release due to combustion and the accompanying pressure increase in the combustion chamber drive a fraction of the hot combustion products out of the chamber. This lowers the pressure in the system until the combustion chamber pressure is below that maintained in the intake fuel and air lines. When this negative pressure differential occurs, some fresh air and fuel is introduced into the combustion chamber. Not all of the residual reaction products are flushed out of the system. In order for spontaneous reignition of the fresh reactants to occur, enough hot reaction products must remain to raise the temperature of the reactants to a point where they will themselves be able to ignite. This reignition then provides the heat release to drive another combustion cycle.

There are several physical and chemical processes which are of particular importance in this system. One concerns the mixing of the inducted fresh fuel and air with the hot reaction products. The spatial orientation of the intake fuel and air lines, the relative pressures which can be maintained in those intake lines, and the geometry of the mixing region of the combustion chamber are all known to play roles in the behavior of the pulse combustor. This turbulent mixing process is not well characterized at present and is a serious limitation to a more complete understanding of the operation of the pulse combustor. A second problem involves a description of the fluid and wave motions in the combustion system, driven by the gas ignition but influenced by many other factors. Recent progress has been made in our ability to model this portion of the combustion system [8].

A third key part of the overall combustor performance is the chemical process of reignition. Clearly the reignition and subsequent burnup of the fuel-air mixture must be complete within some fraction of the total cycle time, or combustion would proceed out into the exhaust system, which is not observed. The very fact that pressure oscillations occur is a further indication that the heat release must be complete within a rather small fraction of the cycle time. This is evident because the combustor is open at the exhaust end to the atmosphere, so if the combustion is slow, then very small pressure waves would be sufficient to maintain a relatively uniform pressure. The present work attempts to compute the rate of ignition in the combustion chamber, making certain simplifying assumptions in order to make the kinetic problem tractable

Regardless of the details of the mixing of the fresh fuel, fresh air, and products of the previous combustion cycles, it is assumed that under

normal operating conditions, reignition during each cycle will occur in the combustor at the location where the ignition process is most rapid. Following the ignition at one location, a combination of flame propagation and later ignitions at other points will occur very rapidly, consuming the great majority of the remaining fuel charge and driving the fluid flow associated with pulsating combustion. Therefore, this kinetic analysis focuses on the time history of the ignition of a single fluid element. It assumes that the mixing of fresh reactants and residual products is instantaneous and complete down to a microscopic level, and that the ignition of the individual fluid element is not affected by interactions with neighboring fluid elements. This then represents a simulation of reignition under the most ideal of conditions. The behavior of an actual system will approximate this ideal system to some extent, and the comparison between the experimental data and the idealized model will provide information on the actual processes of importance.

A working hypothesis is made that the operation of the pulse combustor is kinetically limited. Characteristic reignition time scales calculated as described below on the basis of this hypothesis are then compared with experimental time scales of the pulse combustor operation. In those cases where the model predictions and analysis give good agreement with measured results, it can be concluded that the operation in those cases may indeed be kinetically controlled. Furthermore, the model can then be used in a predictive way to estimate system response to changes in operating conditions such as equivalence ratio, pressure, fuel composition, and others. In the remaining cases where the kinetic model analysis provides trends which are inconsistent with experimental results, it can be concluded that the combustor operation is controlled by physical and/or chemical processes other than chemical kinetics.

SYSTEM PARAMETERS

Three independent parameters have been used to characterize the model system. The first of these is the composition of the fuel itself. Three fuels have been investigated, including methane, mixtures of methane with ethane (as simulated natural gas), and propane. For each fuel, the second system parameter is the fuel/air equivalence ratio Φ, the ratio of actual fuel concentration to that required to consume all of the available oxygen. The third variable in the analysis is the mixing ratio f, defined as the mass fraction of fresh fuel and oxidizer in each sample of igniting gas. Since a given sample of gas, before it has begun to reignite, consists of a mixture of fuel, air, and product species from previous cycles, the mass fraction of residual hot products in the reacting sample is (1-f). Note that f is a mass fraction, not a volume or mole fraction; since the reactants are initially at room temperature and are then heated to temperatures well in excess of 1000 K, the corresponding mole or volume fractions of fresh reactants will be considerably larger than their corresponding mass fractions.

INITIAL CONDITIONS

The adiabatic flame temperature T_{ad} of any given mixture, assuming that there is no significant heat loss, is a function of the fuel composition and the equivalence ratio Φ but is not a function of the mixing fraction f. Therefore, once the fuel and Φ are selected, T_{ad} is uniquely determined. Then for any value of mixing fraction, the instantaneous mixture temperature T_o, before any reactions have taken place, can be calculated by conservation of enthalpy

$$\left[\int_{300\,K}^{T_o} m\,C_p\,dT\right]_{fuel+air} = \left[\int_{T_o}^{T_{ad}} m\,C_p\,dT\right]_{residual\ products}$$

where the masses of fuel and air are related to the mass of products by

$$m_{fuel+air}/(m_{fuel+air} + m_{products}) = f$$

The specific heat c_p for each species is given in the model as a power series in temperature

$$c_p = \sum_{k=0}^{5} a_k T^k$$

and the masses of fuel, air, and products are specified from a knowledge of Φ and f. A very simple iterative technique is used to evaluate T_o from the above relations.

The initial mixture composition is given simply by combining a fraction f of the fresh mixture (in which the relative amounts of fuel, oxygen, and nitrogen are related by Φ and the ratio of nitrogen to oxygen in normal air, assumed to be 3.76 in these models) with a fraction (1-f) of the residual combustion products from the previous cycle, converted to mole fractions for convenience in the model. The initial pressure of the mixture is assumed to be atmospheric. This completes the characterization of the initial conditions, with the pressure, temperature T_o and composition given.

Using these initial conditions and the chemical kinetic reaction mechanism from Table I, the HCT program was used to compute the time required for autoignition of the gas sample. This time τ can be defined in a number of ways, but the most straightforward and physically sensible definition is the time at which the maximum temperature (and pressure) gradient occurs. An example is given in Figure 1 for a mixture of methane

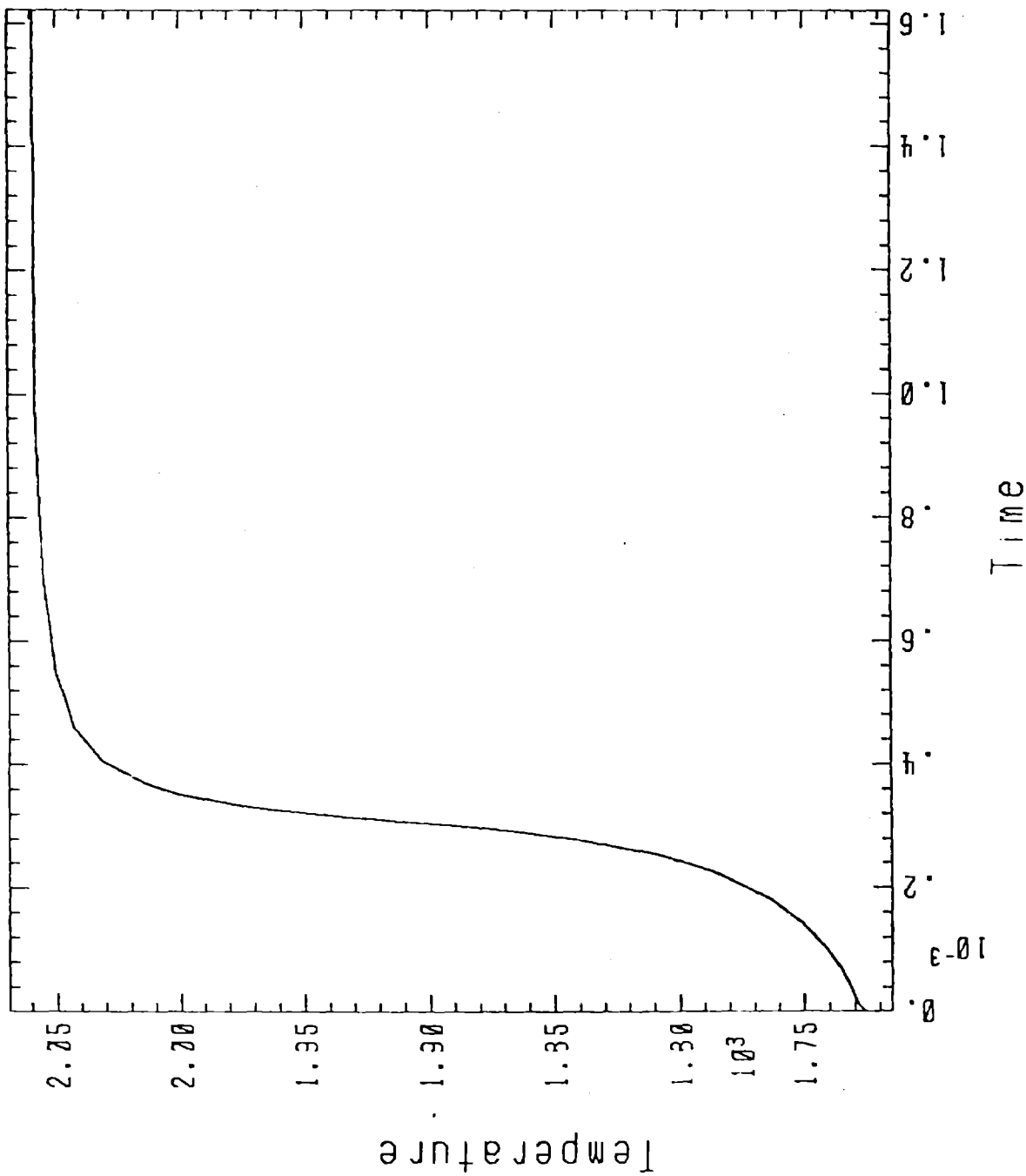

Figure 1

Temperature evolution for case with ϕ = 1.3, f = 0.2.

and air with $\Phi = 1.3$ and $f = 0.2$. The adiabatic flame temperature is calculated to be 2059 K, and the resulting mixture temperature T_o is 1725 K. As seen from Figure 1, the ignition delay time is found to be approximately 0.32 msec. Note that there is still a significant amount of heat release at times later than τ.

RESULTS

The remainder of the modeling analysis consists of relating the computed values of τ to characteristic time scales for the pulse combustor operation. The computed results for methane-air mixtures are summarized in Figures 2 and 3, showing contours of constant Φ in the one case, and contours of constant τ in the other case. Values for $\Phi \geq 1$ are not shown, but in a manner analogous to the variation of burning velocity with Φ, the computed results for $\Phi = 1.5$ are very similar to those for $\Phi = 0.5$ in Figure 2. The minimum ignition delay times occur for $\Phi \approx 1$, with values for $1 \leq \Phi \leq 1.5$ lying continuously between these limits.

The shapes of these curves are quite simple to understand. At constant equivalence ratio Φ, the value of T_o falls steadily as f increases, since the product temperature T_{ad} is constant and more cold reactants are being added to a decreasing amount of hot products. The ignition delay time τ is an exponential function of $(-E_a/T_o)$, with an effective activation energy in excess of 40 kcal/mole [9,10]. Therefore τ will increase rapidly as the mixing fraction f grows.

In all of the available experimental results, a lean limit for methane-air was observed at $\Phi \approx 0.5$. From Figure 2, the contour for $\Phi = 0.5$ indicates a value of $\tau = 1$ msec at $f = 0$. In order to relate this

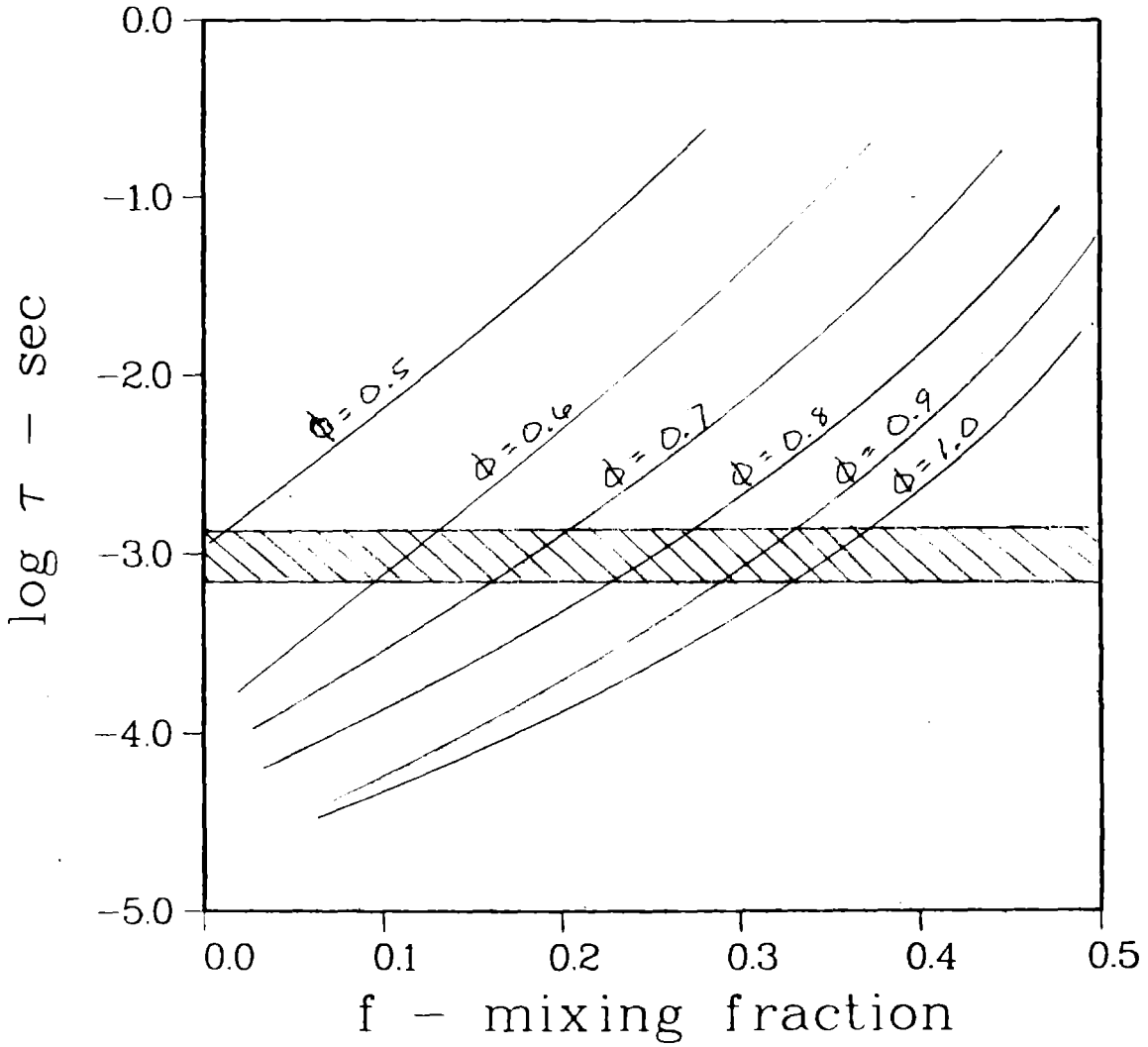

Figure 2

Contours of constant equivalence ratio with varying ignition delay time as a function of mixing fraction. The shaded band represents the suggested optimum operating range of the pulse combustor.

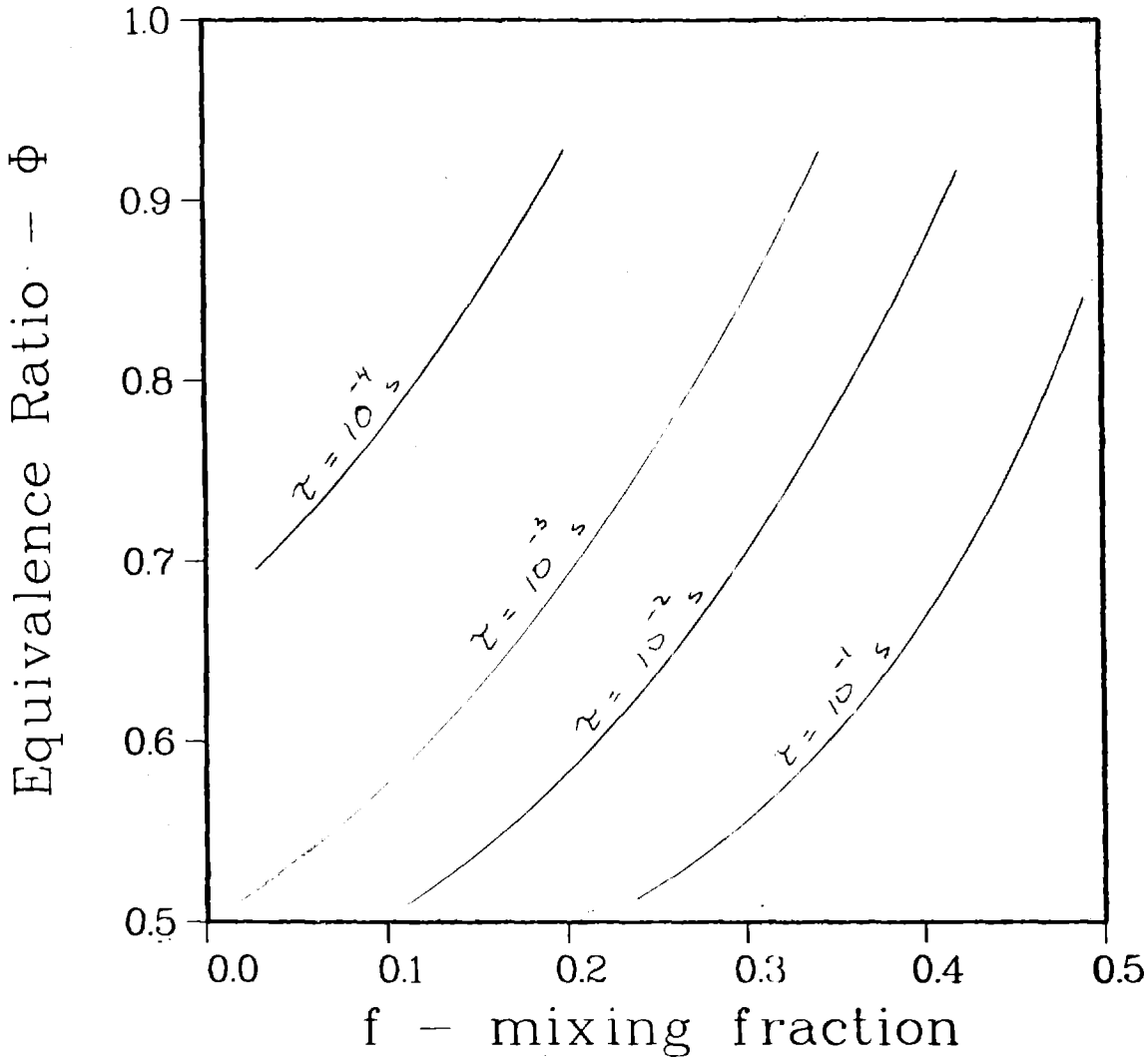

Figure 3

Computed contours of constant ignition delay time in methane-air mixtures, with definitions of f and τ from the text.

to the pulse combustor, it is necessary to recall that these systems have a very well-defined operating frequency which is generally believed to be controlled largely by the acoustic properties of the combustion chamber and exhaust system. For most systems this frequency is in a range of 40 - 200 Hz. It is also reasonable to assume that, during successive reignition, the ignition delay time will be somewhat less than the total cycle time as discussed earlier, since some time is required for subsequent flame propagation, product flow out through the exhaust system, and the intake of fresh reactants.

The intersection of the $\Phi = 0.5$ curve in Figure 2 with 1 msec at $f = 0$ provides an estimate of a critical value of τ for this particular system. It can be assumed then that for these mixtures, a value of τ which is significantly greater than 1 msec will result in unstable or no operation of the pulse combustor, since the time required for reignition is too long. Allowing for a variability in operation and uncertainties in computed results of a factor of 2, a band has been drawn in Figure 2 about this limiting value of τ.

The interpretation of the model results in terms of this limiting band relies very heavily on the need for the combustor to operate at a nearly constant frequency and an assumption that the reignition time remains an effectively fixed fraction of that operating period. If the ignition of a given mixture is too rapid (i.e. a shorter time than that indicated in Figure 2), then the system will adjust by drawing a larger amount f of fresh reactants into the combustion chamber. Because this lowers T_o, the next ignition delay time will be longer, leading to a value of τ which is closer to the optimal value of 1 msec. Conversely, too long a time delay will lead to a reduced fraction f of fresh reactants and a subsequent

reduction in τ. In this sense, the band at τ = 1 msec represents a region of stability, with the dynamics of the reignition and intake processes tending to maintain that stability.

Only for mixtures with Φ less than the lean limit or greater than the rich limit does this feedback mechanism lead to extinction. In these cases the ignition delay time is above the shaded band in Figure 2. However, the reduction in the mixture fraction f to provide smaller values of τ cannot continue because the limiting value of f = 0 is achieved before τ is sufficiently reduced.

RICH LIMIT OF OPERATION

One operating parameter which varies qualitatively from one pulse combustor to another is the rich limit. The pulse combustor at Battelle Columbus [2] indicates a rich limit close to Φ = 1, while another pulse combustor being studied at Sandia Laboratories [11] finds a limit much closer to Φ = 1.5. From Figure 2 and the corresponding results for $\Phi \geq 1$, it is evident that the model predicts that there should be no kinetically controlled rich limit at $\Phi \lesssim 1$. The lean limit of $\Phi \approx 0.5$ and a rich limit of $\Phi \lesssim 1.5$ are predicted by the present approach, so some other mechanism must be responsible for the rich limit of $\Phi \lesssim 1$ encountered in the Battelle Columbus system.

Even though the kinetic model predicts no limit at $\Phi \lesssim 1$, a possible interpretation of this problem is still provided by the present purely kinetic arguments. As Φ approaches stoichiometric (Φ = 1), the required mixing fraction f becomes quite large, between 0.3 and 0.4. Taking into account the fact that f is a mass fraction, for $f \geq 0.3$ well over half of the reacting volume consists of fresh reactants. Therefore a great deal of mixing would have to occur very rapidly in order to achieve the required

initial conditions consistent with stable operation. This suggests strongly that this type of rich limit is due to difficulties in the rate of fuel and air intake, as well as limiting rates of mixing with hot residual products in the combustion chamber. Since the mechanics and geometry of the intake and mixing sections of different pulse combustion systems can vary considerably, it is not surprising that some such systems will experience a mixing-limited rich limit while others with different intake systems will not be explicitly mixing limited in the same way.

EFFECTS OF FUEL TYPE

Methane is well known to exhibit ignition delay times substantially longer than other n-alkane fuels [10] or mixtures of methane and other fuels such as ethane or propane [6, 7, 12, 13, 14] which are commonly present in natural gas. Model computations were carried out for a series of propane-air mixtures and the results compared with those for methane-air mixtures. At each value of Φ and f, values of τ were found to be significantly smaller than those computed with methane as the fuel (Figures 2 and 3). Retaining a limiting value of $\tau \approx 1$ msec for stable operation, the model predicts a lean limit for propane of $\Phi \approx 0.35$. At this time it is not clear whether or not this difference in the lean limit could actually be exploited experimentally, since as pointed out by Keller [15], the intake process will change as the fuel is changed from methane to propane, even though all of the physical equipment in unchanged. That is, because propane is so much larger a molecule than methane, a much smaller mass and volume of propane is needed to provide the necessary fuel for the oxygen. An inlet jet of propane at $\Phi = 0.35$ will not possess the same momentum, energy, and mixing rate as an inlet jet for methane at $\Phi = 0.5$.

Although the use of propane as a fuel may not be as directly relevant to current pulse combustion practical applications as methane or natural gas, some experimental analysis of propane in existing pulse combustors seems likely to be instructive in shedding light on the relative roles of mixing and kinetics.

An alternative means of changing the methane ignition delay time without significantly changing the intake properties is to add small amounts of ethane to the methane. This also provides a fuel mixture which is nearer to natural gas than is pure methane. As noted earlier, both experimental studies and modeling analyses have shown that the presence of small amounts of ethane, propane and certain other fuel molecules, in quantities as small as 2-5% of the fuel, can have a quite dramatic effect on the ignition properties of the mixture. Computations found that the replacement of approximately 15% of the methane fuel with ethane resulted in a shift in the lean limit of operation of $\Delta\Phi = 0.05$. That is, if the lean limit is $\Phi = 0.5$ for methane-air, the lean limit in the same system for a fuel consisting of 85% CH_4-15% C_2H_6 would be $\Phi = 0.45$. Consistent with other ignition studies in methane-ethane mixtures, the addition of a small amount of ethane has a large effect, while addition of further ethane has a gradually smaller influence.

EFFECTS OF DILUTION

A further method of influencing the ignition delay time, and therefore the operating limits of the pulse combustor, is by adding inert diluents to the fresh mixtures. Dilution by species such as CO_2 or H_2O has been shown [16,17] to reduce the rates of ignition of both hydrogen-air and hydrocarbon-air mixtures. The present model was used to examine the

effects of dilution by the addition of CO_2. It was found that when 10% of the incoming fuel and air was replaced by CO_2, the ignition delay time of a Φ = 0.7 methane-air mixture with f = 0.1 was increased from 0.19 msec to 1.98 msec, an increase of an order of magnitude. Other inert additives were found to be somewhat less effective, with the addition of 10% additional N_2 to the same Φ = 0.7 mixture increasing τ to 0.87 msec. In the case of dilution by inert species, the mechanism for the delay is simply related to the fact that the inert species absorbs some of the thermal energy from the reaction of the hydrocarbons, so the product adiabatic flame temperatures and the initial mixture temperatures are both reduced. This is in distinct contrast to the case of sensitization of methane ignition by addition of ethane or propane or the opposite case of kinetic inhibition by the addition of selected halogenated species [18], both processes which are primarily kinetic in nature rather than thermal as in the case of dilution by inert species.

PHYSICAL SYSTEM MODIFICATION

If the operating limits to composition which can support normal pulse combustor performance can be related to ignition delay times in the way described above, then the results of Figure 2 suggest another possible strategy for slightly modifying the lean limit. The stability limit, the shaded band at τ = 1 msec, is assumed to be a fixed fraction of the natural period of the pulse combustor. If that fraction remains constant as the geometry of the pulse combustor is changed, then acoustic changes in the combustion chamber to decrease the pulse frequency (increase the time interval between successive reignitions) might result in a small reduction in the lean limit for stable operation. Conversely, an increase in the

acoustically determined operating frequency of an order of magnitude would result in a shift in the lean limit from $\Phi = 0.5$ to a higher value of approximately $\Phi = 0.6$.

CONCLUSIONS

The simple characteristic time analysis described in this paper must be considered within the context of current research on pulse combustors. On the one hand, this type of analysis is deceptively powerful alone, identifying the key system parameters and physical processes which control the combustor performance, even in those situations where the chemical kinetic factors are not limiting. The predictions about modifications of the operating limits, primarily the lean equivalence ratio limit, need testing in experiments, but if they can be confirmed, then the simple model becomes a useful practical tool as well as an academic tool for system analysis. On the other hand, it is unrealistic to push too hard on a simple submodel which deals with only one of the many physical and chemical processes which occur. Eventually it will become necessary to assemble a much more complete detailed overall model of the pulse combustor, including fluid mechanics in multidimensional geometry, heat transfer, turbulence, and other complex and interconnected problems. The present chemical kinetics modeling work represents the one submodel which is probably the most highly developed currently, one which will be available for incorporation into a more complete total model at some time in the future.

ACKNOWLEDGMENTS

Valuable discussions with J.M. Corliss, B.T. Zinn and J.O. Keller are greatly appreciated. This work was performed under the auspices of the U.S. Department of Energy by the Lawrence Livermore National Laboratory under contract No. W-7405-ENG-48. Financial support for this work was provided by the Gas Research Institute, J. A. Kezerle, Manager of Basic Combustion Research.

REFERENCES

1. Lund, C.M., "HCT- A General Computer Program for Calculating Time Dependent Phenomena Involving One-Dimensional Hydrodynamics, Transport, and Detailed Chemical Kinetics", Lawrence Livermore National Laboratory report UCRL-52504 (1978).

2. Battelle, Columbus Laboratories Annual Report, Gas Research Institute report GRI 85/0029, April 1985.

3. Pitz, W.J., Westbrook, C.K., Proscia, W.M., and Dryer, F.L., "A Comprehensive Chemical Kinetic Reaction Mechanism for the Oxidation of n-Butane", Twentieth Symposium (International) on Combustion, in press (1985).

4. Westbrook, C.K., and Pitz, W.J., "A Comprehensive Chemical Kinetic Reaction Mechanism for Oxidation and Pyrolysis of Propane and Propene", Combust. Science and Technol. 37, 117 (1984).

5. Westbrook, C.K., Creighton, J., Lund, C., and Dryer, F.L., "A Numerical Model of Chemical Kinetics of Combustion in a Turbulent Flow Reactor", J. Phys. Chem. 81, 2542 (1977).

6. Westbrook, C.K., "An Analytical Study of the Shock Tube Ignition of Mixtures of Methane and Ethane", Combust. Science and Technol. 20, 5 (1979).

7. Westbrook, C.K., and Pitz, W.J., "Effects of Propane on Ignition of Methane-Ethane-Air Mixtures", Combust. Science and Technol. 33, 315 (1983).

8. Dwyer, H.A., Bramlette, T.T., Keller, J.O., and Sanders, B.R., "A Numerical Model of a Pulse Combustor", Proceedings of the 10th International Colloquium on Dynamics of Explosions and Reactive Systems, in press (1985).

9. Burcat, A., Scheller, K., and Lifshitz, A., "Shock Tube Investigation of Comparative Ignition Delay Times for C_1-C_5 Alkanes", Combust. Flame 16, 29 (1971).

10. Westbrook, C.K., and Pitz, W.J., "Chemical Kinetics Modeling of the Influence of Molecular Structure on Shock Tube Ignition Delay", Proceedings of the 15th International Symposium on Shock Waves and Shock Tubes, in press (1985).

11. Keller, J.O., Saito, K., and Kishimoto, K., "An Experimental Investigation of a Pulse Combustor -- Flow Visualization by Schlieren Photography", presented at the 1984 Fall Meeting of the Western States Section of the Combustion Institute, October 1984.

12. Crossley, R.W., Dorko, E.A., Burcat, A., and Skinner, G.B., "The Effect of Higher Alkanes on the Ignition of Methane-Oxygen-Argon Mixtures in Shock Tubes", Combust. Flame 19, 373 (1972).

13. Eubank, C.S., Rabinowitz, M.J., Gardiner, W.C., Jr., and Zellner, R.E., "Shock Initiated Ignition of Natural Gas-Air Mixtures", Eighteenth Symposium (International) on Combustion, p. 1767, The Combustion Institute, Pittsburgh (1981).

14. Vandermolen, R., and Nicholls, J.A., "Blast Wave Initiation Energy for the Detonation of Methane-Ethane Mixtures", Combust. Science and Technol. 21, 75 (1979).

15. Keller, J.O., private communication (1985).

16. Moen, I.O., Ward, S.A., Thibault, P.A., Lee, J.H., Knystautas, R., Dean, T., and Westbrook, C.K., "The Influence of Diluents and Inhibitors on Detonations", Twentieth Symposium (International) on Combustion, in press (1985).

17. Shepherd, J.E., "Chemical Kinetics of Hydrogen-Air-Diluent Detonations", Proceedings of the 10th International Colloquium on Dynamics of Explosions and Reactive Systems, in press (1985).

18. Westbrook, C.K., "Inhibition of Hydrocarbon Oxidation in Laminar Flames and Detonations by Halogenated Compounds", Nineteenth Symposium (International) on Combustion, p. 127, The Combustion Institute, Pittsburgh (1983).

LEGAL NOTICE